Isothermal Crystallization of Polyethylene Oxide/Silver Nanoplate Composites

Nandho Rahmansyah,[1] Chieh-Tsung Lo,[1] Ciou-Mei Syu,[2] Chien-Liang Lee[2]

[1]*Department of Chemical Engineering, National Cheng Kung University, Tainan City 701, Taiwan*
[2]*Department of Chemical and Material Engineering, National Kaohsiung University of Applied Sciences, Kaohsiung 807, Taiwan*

Received 29 July 2010; accepted 28 January 2011
DOI 10.1002/app.34244
Published online 21 May 2011 in Wiley Online Library (wileyonlinelibrary.com).

ABSTRACT: This research was accomplished to investigate the kinetics of isothermal crystallization of polyethylene oxide (PEO)/silver nanoplate composites. It was obtained that the spherulites increased in size and numbers with time for the composites with various particle loadings. Additionally, the spherulite growth rate of composites decreased with an increase in the crystallization temperature and increased with the addition of nanoplates. The spherulite growth rate was further analyzed by the theory developed by Lauritzen and Hoffman. The product of the lateral surface free energy (σ) and the end surface free energy (σ_e) decreased with an increase in the content of nanoplates. We proposed the possible crystallization mechanisms of these PEO/nanoplate composites according to the change of σ and σ_e with the presence of nanoplates. A controlled experiment showed a minor change in PEO crystallization with the presence of a surfactant C_{16}TAB. This implied that the unique size and shape of nanoplates plays a key role on hindering the primary nucleation of PEO and increasing the spherulite growth rate. © 2011 Wiley Periodicals, Inc. J Appl Polym Sci 122: 1236–1244, 2011

Key words: nanocomposites; crystallization; spherulites; nanoplates; polyethylene oxide

INTRODUCTION

Much research has been done to understand the isothermal crystallization of polymer nanocomposites. These polymer composites consist of a new class of fillers and they are categorized in three main groups depending on the fillers' geometry, including polymer/nanoclays, polymer nanofibers, and polymer/nanoparticles.[1] The study of these composites is to elucidate the effect of these fillers on the crystallization behavior of these composites as compared with neat polymer.

The study of crystallization in polymer/clay nanocomposites was complicated due to the interplay between the dispersion of clay reinforcement within a polymer matrix and the extent of intercalation versus exfoliation of the reinforcement phase. Differences in polymer/filler miscibility and filler dispersion can have significant effects on the nucleation rate, overall crystallization kinetics, and crystal morphology. Fornes et al. showed that the kinetics of polymer crystallization increase significantly at very low clay content whereas the overall crystallization is retarded at high clay loading.[2] In addition, the higher crystallization rate could be achieved for nylon-6 with higher molecular weight due to its greater extent of exfoliation. The crystallization behavior of polyethylene oxide (PEO)/clay nanocomposites was reported by Strawhecker.[3] It was noted that the presence of clay hinders PEO crystallization as observed by the decrease in the crystallization temperature. However, the overall crystallization rate becomes faster in the composites as compared with the neat polymer. This observation was attributed to the large number of crystallites created in the presence of clay. However, this result contradicts to other work on polymer/clay nanocomposites and was attributed to the presence of specific interactions between PEO and clay, resulting in the formation of amorphous PEO in the vicinity of clay layers.

In the study of polypropylene/single-walled carbon nanotube (PP/SWCNT) composites, Bhattacharya et al. showed higher isothermal crystallization rate, narrower crystallization and melting peaks, and smaller spherulite size with the addition of nanotubes.[4] The changes in the crystallization behavior and the spherulitic morphology were caused by the enhanced nucleation of PP in the presence of SWCNT. Valentini et al. reported that the presence of SWCNTs enhanced the nucleation process and showed saturation at low nanotube concentration.[5] The kinetics of crystallization was strongly affected

Correspondence to: C.-T. Lo (tsunglo@mail.ncku.edu.tw) and C.-L. Lee (cl_lee@cc.kuas.edu.tw).

Contract grant sponsor: National Science Council in Republic of China; contract grant numbers: NSC 97-2221-E-006-024, NSC 98-2221-E-151-033-MY2.

by the distance between nanotube bundles. The presence of nanotubes also decreased the size of the spherulites in PP/SWCNT composites. In melt-mixed PP/SWCNT composites, Manchado et al. showed that the crystallization rate of PP increased, but no substantial change was observed in the crystalline form of PP.[6]

In three dimensional fillers, Kennedy et al. studied the crystallization of poly(propylene oxide) and isotactic polystyrene with the addition of silica particles.[7] At low particle loadings, the fillers acted as a nucleation agent, thus greatly enhancing the overall crystallization rate but also significantly reducing the spherulite growth rate. This trend was attributed to the adsorption of polymer chains on filler surfaces, which increased the viscosity and consequently decreased the transport of crystallizable segments to the crystal growth front. In contrast, Burke et al. observed an increase in the crystallization rate of TiO_2-filled PP, but they did not find any change in the spherulite growth rate.[8] Similar results were obtained by Raimo et al. in which the addition of TiO_2 particles to ethylene-propylene copolymer promoted the nucleation.[9] At a high crystallization temperature, the spherulite growth rate was unchanged whereas at a low crystallization temperature the spherulite growth rate was higher than that of neat copolymer. Wang et al. showed that the manipulation of the interfacial properties of $BaSO_4$ microparticles using different chemical modifiers could alter the interfacial interaction between PP and $BaSO_4$ and hence the PP spherulite growth rate.[10] The addition of weakly interacting fillers decreased the spherulite growth rate. In contrast, the strongly interacting PP/$BaSO_4$ system resulted in an even slower rate due to the confinement effect of polymer chains introduced by the attractive interaction at the polymer/filler interface. Yang et al. investigated the isothermal crystallization of Nylon 6/SiO_2 nanocomposites prepared by *in situ* polymerization.[11] The presence of unmodified silica particles increased the crystallization rate. In contrast, the crystallization rate slightly decreases with the content of modified silica particles. This observation was attributed to the acceleration of crystallization owing to the enhanced nucleation in the case of unmodified silica. On the other hand, good adhesion between silica and polymer impedes the motion of polymer chains and therefore prevents the crystallization.

Large amount of research focuses on the isothermal crystallization of polymer/micron-sized particle and polymer/nanosphere composites with respect to the spherulite diameter, spherulite growth rate, and the morphological development of polymer crystals. In contrast, less research focuses on the crystallization kinetics of polymer/nanoplate composites. In this work, we prepared silver nanoplates in PEO to study the crystallization of PEO/nanoplate composite. This is the newly developed nanocomposites with nanometer-sized particles in a plate form. Our goal is to understand the effect of silver nanoplates on the isothermal crystallization of PEO. The isothermal crystallization was investigated by using optical microscopy (OM) and was analyzed by Lauritzen-Hoffman's theory.

Lauritzen-Hoffman's theory

The Lauritzen-Hoffman's theory describes the kinetics of crystallization in molecular terms for linear flexible polymers that are crystallized from the melt into the chain folded lamellae.[12] This theory and its various modifications constitute widely used methodology to interpret and simulate the crystallization of a large number of polymers.[13–17] Although this theory is suited the best to describe the chain folded crystallization of flexible polymers, it has also been applied to model the crystallization of other more rigid chain systems, such as PEEK.[18]

The Lauritzen-Hoffman's theory leads to a calculation involving the lateral substrate completion rate, S_T, given by eq. (1)[19]

$$S_T = \frac{1}{l_u} \int_{2\sigma_e/\Delta G}^{\infty} S(l)dl \tag{1}$$

where l_u is the monomer length, ΔG is the total free energy, σ_e is the end surface free energy, l is the lamellar thickness, and S(l) is the subsequent flux of stem length for deposition. This allows for calculating the rate of stem deposition (i), i.e., the surface nucleation rate in terms of stems (s^{-1} cm^{-1}) by the following relation[19]

$$i = \frac{S_T}{L} = \frac{S_T}{n_1 a_0} \tag{2}$$

where n_1 is the number of stems with a width of a_0 that makes up the substrate of length L. The second important parameter leading to the crystal growth rate (G) is given by the substrate completion rate (g)[19]

$$g = a_0(A - B) \tag{3}$$

where A and B are rate determining steps. Both the substrate nucleation rate and substrate completion rate decide the crystal growth rate and the exact nature of this relation is given by the relative rate of i versus g.[19–21]

Three regimes are considered in polymer crystallization. In Regime I,[20,21] the growing nucleus sweeps completely across the crystalline interface before any new nuclei appear. In Regime II,[20,21] the relative rate

of i and g is similar. This allows the new nuclei to form even before the previous layer is completely filled. In Regime III,[22,23] a large number of nuclei occurs and hence little or no substrate completion takes place. These three regimes were experimentally observed in a variety of polymer systems and the supercooling dependency of the growth rate in accordance with the above analysis was confirmed.

The substrate nucleation rate and completion rate are given by[19]

$$i = \frac{N_0\beta}{n_l a_0 l_u}\left[\frac{kT}{2b_0\sigma} - \frac{kT}{2b_0\sigma + \Delta G}\right]\exp\left[\frac{-4b_0\sigma_e\sigma}{\Delta G k T}\right] \quad (4)$$

$$g = a_0\beta\left[1 - \exp(\frac{a_0 b_0 \delta\Delta G}{kT})\right]\exp\left[\frac{-2a_0 b_0\sigma_e}{kT}\right] \quad (5)$$

where N_0 is the number of initial stems, b_0 is the layer thickness, σ is the lateral surface energy, δ is the increment above the minimum lamellar thickness, k is the Boltzmann constant, and T is the crystallization temperature. β can be obtained by the Vogel-Fulcher or Arrhenius expressions. For crystallization from dilution solution, this factor is described in the Arrhenius expression[19]

$$\beta = G_0\exp\left[\frac{-\Delta E}{RT}\right] \quad (6)$$

Here, G_0 is the pre-exponential factor, ΔE is the Arrhenius activation energy, and R is the gas constant. These equations give the crystal growth rate as[19]

$$G = G_0\exp\left[\frac{-\Delta E}{RT}\right]\exp\left(-\frac{K_g}{T\Delta T_c f}\right) \quad (7)$$

where

$$K_g = \frac{nb_0\sigma\sigma_e T_m}{k\Delta H_f} \quad (8)$$

Here, K_g is the nucleation constant in which n is 4 for Regimes I and III and 2 for Regime II. G_0 is the pre-exponential factor, ΔT_c is the degree of unercooling ($\Delta T_c = T_m - T$), T_m is the equilibrium melting temperature of polymer, $f = 2T/(T_m + T)$ is the correction factor, and ΔH_f is the heat of fusion of a perfect crystal. In addition, the work of chain folding can be derived from the end surface free energy by[19]

$$q = 2\sigma_e A_0 \quad (9)$$

where A_0 is the cross-sectional area of the chain.

The nucleation constants, K_g, and G_0 can be obtained by a *L-H* plot from eq. (7) in the form of $[ln(G) + \Delta E/RT]$ versus $[1/T\Delta T_c f]$. The first exponential term in eq. (7), $\exp(-\Delta E/RT)$, indicates the chain transport effect on the interface. The second term, $\exp(-K_g/T\Delta T_c f)$, represents the secondary nucleation effect. The *L-H* plot was also applied to obtain $\sigma\sigma_e$ if both ΔH_f and b_0 of the polymer are known.[24,25]

EXPERIMENTAL

Materials

The polymer used in this work is PEO with the molecular weight of 100,000 g/mol, purchased from Sigma-Aldrich Co.

Synthesis of silver nanoplates

The approach of synthesizing Ag triangular nanoplates was modified from the seed growth method.[26] Initially, a 50 μL of 0.05*M* silver nitrate ($AgNO_3$) aqueous solution was added into a 10 mL of 2.5×10^{-4} *M* sodium citrate aqueous solution. A 25 μL of ice-cold 0.1*M* $NaBH_4$ solution was gradually added into the stirred solution of sodium citrate and $AgNO_3$ and the Ag seed solution was obtained. A 0.6 mL of 0.05*M* $AgNO_3$ was mixed with a 120 mL of 0.1*M* hexadecyltrimethy ammonium bromide (C_{16}TAB) aqueous solution. A 6 mL of 0.1*M* ascorbic acid and 1 mL of the prepared Ag seed solution were slowly dropped into the C_{16}TAB aqueous solution. The triangular Ag nanoplates were then developed after a 0.48 mL of 2*M* NaOH aqueous solution was introduced. As-prepared nanoplates were centrifuged several times to remove the residual chemicals. The nanoplates were redispersed in deionized water for the preparation of nanocomposites.

Preparation of PEO/silver nanoplate composites

To prepare PEO/silver nanoplate composites, different amounts of PEO were dissolved in the Ag nanoplate solution and the composite solution was stored at room temperature for three days to allow for the self-assembly of nanoplates in the PEO matrix.

Transmission electron microscopy

Transmission electron microscopy (TEM) with a Jeol JEM-1200 CXII transmission electron microscope operated on an acceleration voltage of 80 keV was used to characterize the dispersion of Ag nanoplates in PEO.

Optical microscopy

Optical microscopy was carried out with a Nikon H550L Eclipse 50i LV-UEPI microscope in conjunction with a Mettler hot stage (FP-82). Composites were prepared by dropping composite solution on a glass slide to form a specimen with a thickness of

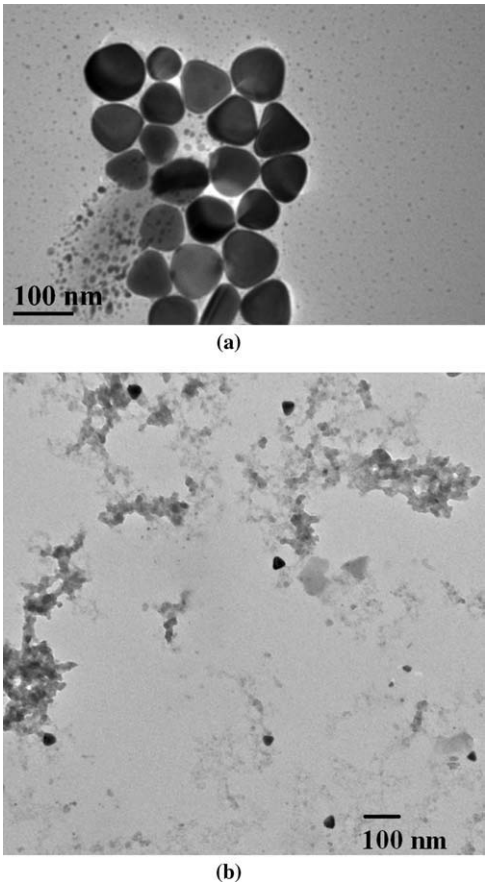

Figure 1 TEM images of (a) silver nanoplates and (b) 4.8 wt % silver nanoplates dispersed in the PEO matrix.

~20 μm. The composite was heated to 100°C and kept for 20 min to remove crystals. Then the temperature was quenched to a crystallization temperature to allow for PEO crystallization. The growth of spherulites was recorded using a Sony color video camera SSC-DC80 Super Exwave, and the spherulite growth rate was measured from time-lapsed frames of spherulitic front.

RESULTS AND DISCUSSION

Silver nanoplates

Figure 1 shows the TEM images of Ag nanoplates. These nanoplates exhibit triangular shape with a mean length of ~84 nm [Fig. 1(a)]. The silver nanoplates in PEO shown in Figure 1(b) reveals good dispersion due to the nature of hydrophilic PEO and the hydrophilic surfactant (C_{16}TAB) tethered on these nanoplates.

Isothermal crystallization of PEO/nanoplate composites

Figure 2 shows the spherulites of neat PEO [Fig. 2(a)] and its nanocomposites [Figs. 2(b–f)] after the impingement of these spherulites. It was obtained that the spherulites of neat PEO have much smaller size whereas those of PEO/nanoplate composites exhibit considerable size. This suggested that the incorporation of silver nanoplates in the PEO enhances the energy barrier for the nucleation of PEO crystals and thus the nucleation rate of nanocomposites decreases, leading to the larger spherulites in composites after the occurrence of spherulite impingement.

Spherulite growth rate

The spherulite growth rate of neat PEO and PEO/silver nanoplate composites were measured by OM. Figure 3 shows the growth of PEO spherulites with 3.6 wt % nanoplates at 48°C with time. The spherulite size of composites was analyzed and is shown in Figure 4. Figure 4 also shows the change in the radius of spherulites with time at various particle loadings. In neat PEO and its composites, the radius of the spherulites increased linearly with time before the occurrence of spherulite impingement. It was proposed that the exclusion of noncrystallizable species from growing spherulites would accumulate at the crystallization growth front and impede the transport of crystallizable species from the melt to the growing edge.[27] This phenomenon causes a deviation of linear spherulite growth after the spherulites reach a certain size. Since no such behavior was observed in both neat PEO and its composites, it could be concluded that the nanoplates were not excluded during the growth of spherulites.

The spherulite growth rate, $G = dR/dt$ where R is the radius of spherulite, was calculated via the slope of the regression line fitted to the experimental data at a given crystallization temperature. Figure 5 shows the averaged spherulite growth rate at different crystallization temperatures and various particle loadings. The spherulite growth rate decreased with an increase in the crystallization temperature. At high temperatures, the degree of undercooling is small. As a result, the nucleation rate reduced, causing the reduction of the overall crystal growth rate. In comparison of the spherulite growth rates of the composites at different particle loadings, the incorporation of nanoplates promoted the growth of spherulites. Thus, the spherulite growth rate of PEO increased with the addition of nanoplates. This result is in good agreement with an increase in the spherulite growth rate of poly(ethylene 2,6-naphthalate) with the incorporation of nanoparticles (the size of particles ~7 nm).[28]

Lauritzen and Hoffman parameters

The parameters in Table I were used to analyze the spherulite growth rate of neat PEO and its

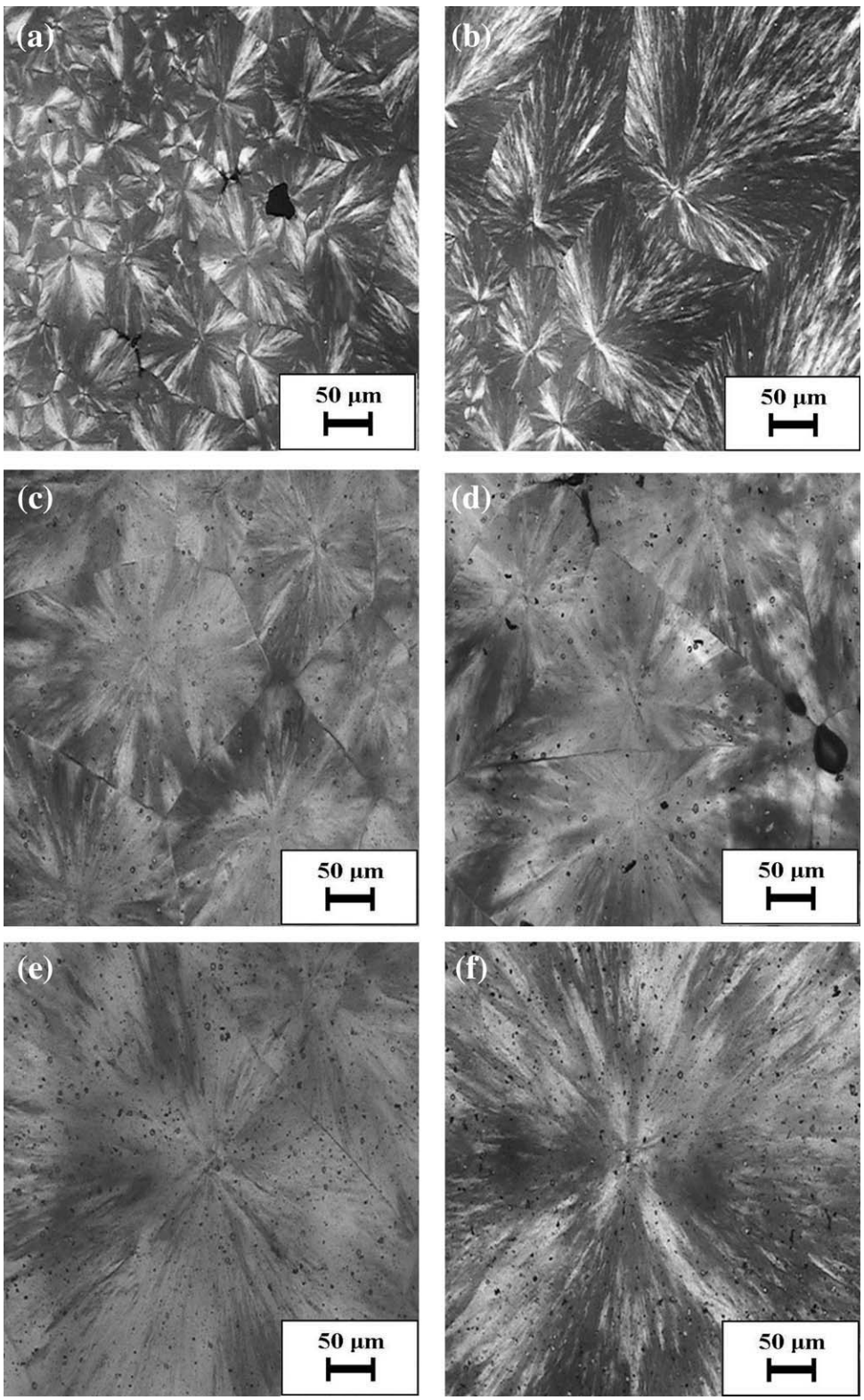

Figure 2 Crystallization of (a) neat PEO; (b) composite with 1.2 wt % nanoplates; (c) composite with 2.4 wt % nanoplates; (d) composite with 3.6 wt % nanoplates; (e) composite with 4.8 wt % nanoplates; and (f) composite with 9.1 wt % nanoplates. Composites were crystallized at 48°C.

composites based on the Lauritzen-Hoffman's theory as shown in eq. (7). Figure 6 was obtained on the basis of the data points in Figure 5. K_g and G_0 values were obtained with respect to the slope and intercept of the fitted linear regression lines (Table II).

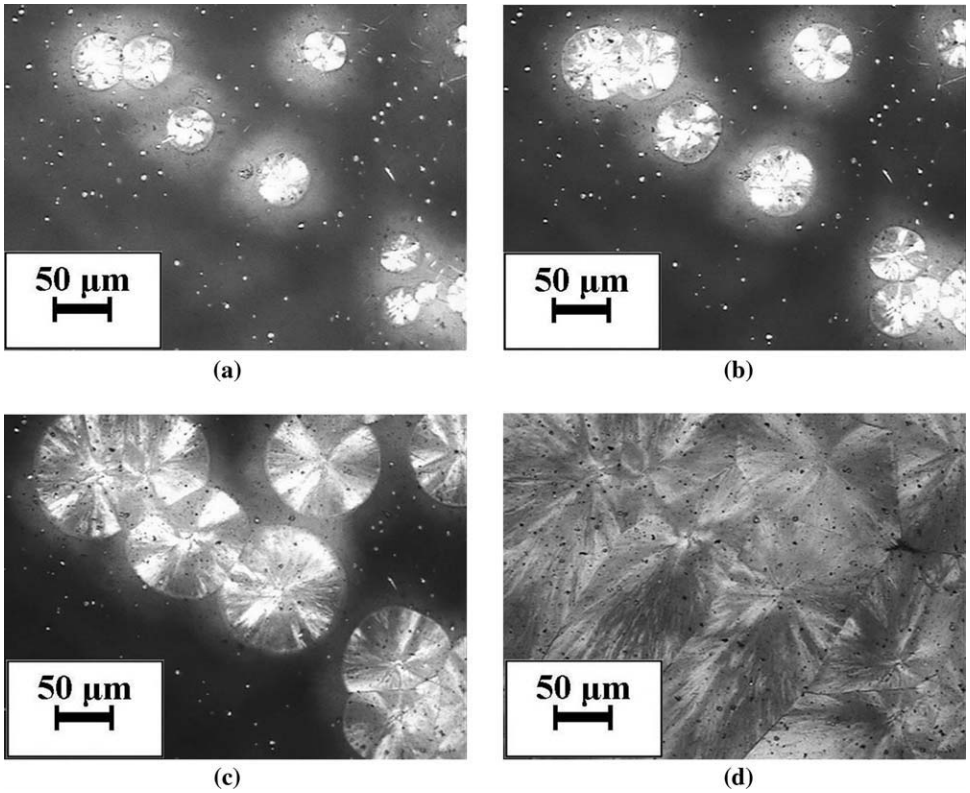

Figure 3 Spherulite growth of PEO with 3.6 wt % of nanoplates at $T = 48°C$ with time (a) 5 s; (b) 10 s; (c) 30 s; and (d) 90 s.

Because the determination of the surface free energy product ($\sigma\sigma_e$) in Figure 6 is complicated by an uncertainty of the crystallization regime, we utilized the Lauritzen Z-test in eq. (10) to distinguish between Regimes I and II, but Regime III is not considered in this approach.[19]

$$Z \approx 10^3 \left(\frac{L}{2a_0}\right)^2 \exp[(-X/(T\Delta T_c))] \qquad (10)$$

Here, $X = K_g$ and $Z \leq 0.01$ for Regime I, whereas $X = 2K_g$ and $Z \geq 1$ for Regime II. As pointed out by Hoffman and Lauritzen[19] and Wang and Nishi,[33] it is more convenient to use the known value of K_g and the inequalities of Z to obtain the values of L in the two regimes and to estimate the realistic of such values. Application of the Z test to the neat PEO and its composites in the entire range of T leads to the following results. If crystallization is in Regime I,

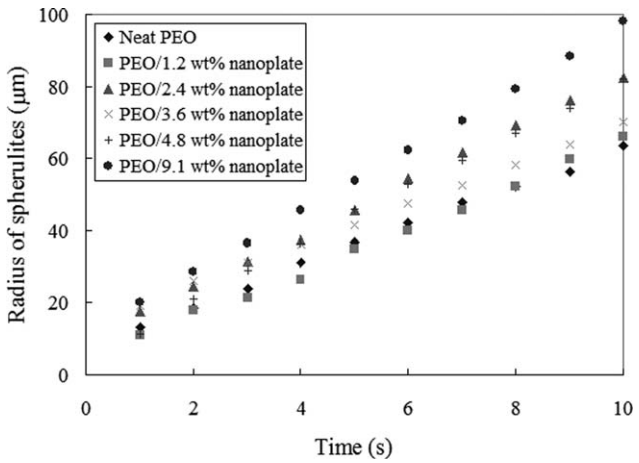

Figure 4 The radius of the spherulites of neat PEO and its composites as a function of time. The crystallization temperature is 43°C.

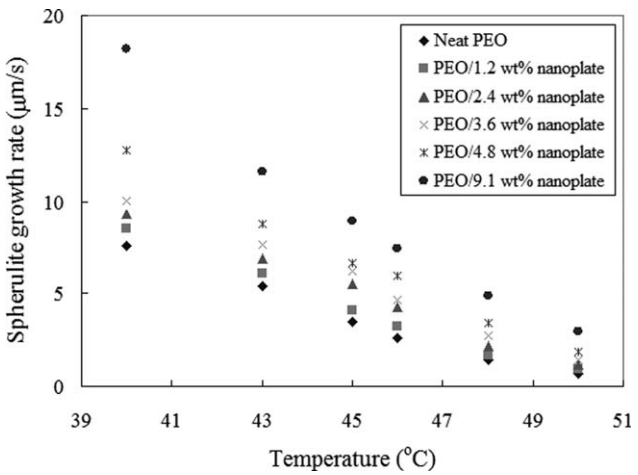

Figure 5 The spherulite growth rate of neat PEO and its composites as a function of crystallization temperature.

TABLE I
Lauritzen and Hoffman Parameters

Parameter	Value	Reference
ΔE	5736 cal/mol	14
T_m	69°C	29, 30
ΔH_f	203 J/g	31
b_0	0.465 nm	32

L is between 0.2 and 2.0 Å at the temperatures of interest for both neat PEO and its composites. This seems to be unrealistic small. In contrast, if crystallization is assumed to be in regime II, $L \geq 22$ Å for both neat PEO and its composites. On the basis of this simple calculation, the crystallization of both neat PEO and its composites follows the Regime II. Within the temperature range that the experiments were performed, the Regime II crystallization of PEO is in good agreement with that proposed by Buckley and Kovacs.[34] They found that the crystallization of low molecular weight PEO is in Regime II in the whole temperature range (*ca.* 30–60°C).

It has to point out that our analysis of the isothermal crystallization of PEO/nanoplate composites is simply based on the universal activation energy for transport (ΔE) for both neat PEO and its composites. This assumption is generally applied to a variety of blend and composite systems.[35–37] However, Abraham et al.[38] characterized dynamic rheological behaviors of PEO/organo clay nanocomposites and reported a change in the activation energy of 5.5% and −40.2% with 2 and 4% volume fraction loadings. In the absence of rheological measurements, a simple calculation was performed to visualize how the varied values of the activation energy would impact on the values of K_g and hence the values of $\sigma\sigma_e$. If the addition of nanoplates caused the 5.5% and −40.2% change in the activation energy of PEO, a change of less than 1% (e.g., from 396 ergs^2/cm^4 for neat PEO to 399 ergs^2/cm^4 for PEO/9.1% nanoplate composite) and −5.5% (e.g., from 396 ergs^2/cm^4 for neat PEO to 374 ergs^2/cm^4 for PEO/9.1% nanoplate composite) in $\sigma\sigma_e$ for all composites was obtained, indicating that the small content of nanoplates would not have significant effect on the diffusion of crystallizable segments. Therefore, the assumption of a universal value of ΔE seems to be reasonable in the PEO/nanoplate composites.

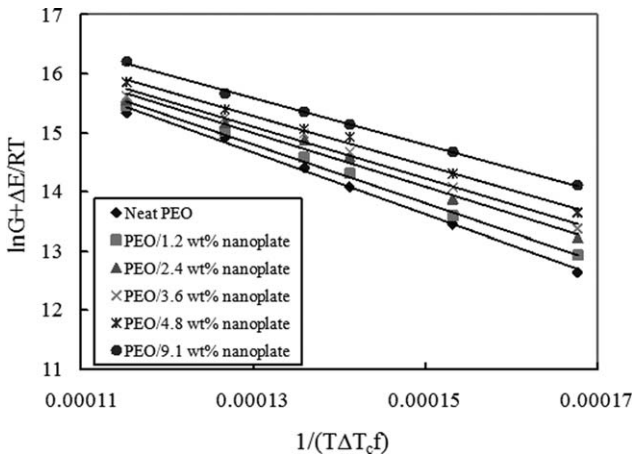

Figure 6 Plots of $[lnG + \Delta E/RT]$ versus $[1/T(\Delta T_c)f]$ for neat PEO and its composites.

TABLE II
Lauritzen and Hoffman Parameters Extracted from eqs. (7) and (8)

Sample	lnG_0 (μm/min)	$K_g \times 10^{-4}$ (K^2)	$\sigma\sigma_e$ (ergs^2/cm^4)
neat PEO	21.5	5.23	523
PEO/1.2 wt % nanoplates	21.3	4.97	497
PEO/2.4 wt % nanoplates	20.9	4.57	457
PEO/3.6 wt % nanoplates	20.8	4.37	437
PEO/4.8 wt % nanoplates	20.8	4.20	420
PEO/9.1 wt % nanoplates	20.7	3.96	396

K_g relates directly to the surface nucleation rate that can be represented by the surface free energy product. It was obtained that K_g decreased with the addition of nanoplates. The incorporation of silver nanoplates reduced the nucleation of PEO and hence caused the creation of the corresponding free polymer crystal surface more dominant than the creation of interface between polymer crystals and substrate. In Table II, $\sigma\sigma_e = 523$ ergs^2/cm^4 in neat PEO. This is within 15% of the value reported by Kovacs et al. (450 ergs^2/cm^4 in the assumption of regime II).[39] The slight difference is presumably due to the different molecular weight of PEO ($M_w = 150$ k) and different expression of β in eq. (6) (Vogel-Fulcher expression) in Kovacs's work.

From the magnitude of $\sigma\sigma_e$, a known value of either σ or σ_e can be employed to calculate the other. However, the lack of σ and σ_e of composite with different nanoplate contents makes it difficult to extract σ and σ_e from $\sigma\sigma_e$. The general approach to analyze σ and σ_e is to input a constant σ and calculate σ_e. Because σ relates to the segmental nature of polymer chains as reflected by the characteristic ratio (C_∞), a constant σ regardless of the filler content indicates that the presence of nanoplates does not cause any chain extension during crystallization. This assumption is generally used in various blend and composite systems.[35,36,40-42] Following this assumption and taking $\sigma = 10$ ergs/cm^2,[30] σ_e reduced from 52.3, 49.7, 45.7, 43.7, 42.0, to 39.6 ergs/cm^2 for 0 wt %, 1.2 wt %, 2.4 wt %, 3.6 wt %, 4.8 wt %, 9.1 wt % nanoplate loadings. The work of chain folding was then related to σ_e by using eq. (9). For $A_o = 0.214$ nm^2,[30] q of the composites varied from 3.22, 3.06, 2.81, 2.69, 2.59, to 2.44 kcal/mol for 0 wt %, 1.2 wt %, 2.4 wt

%, 3.6 wt %, 4.8 wt %, 9.1 wt % nanoplate loadings. The depression in q implied that the silver nanoplates reduced the work required in folding the PEO chains in the nanocomposites. This result is in good agreement with the work reported by Kim et al.[43] that the presence of silica nanoparticles as a filler in the poly(ethylene 2,6-naphthalate) decreased the work required for creating a new polymer crystal surface, leading to the faster growth rate.

Instead of a constant σ for the neat polymer and its composite, Krikorian and Pochan assumed a constant σ_e for organoclay reinforced poly(L-lactic acid) nanocomposites to obtain the relationship between σ and the filler content.[44] This assumption suggested that the free energy of chain folding of the lamellar crystals is independent of the addition of fillers and the presence of nanoplates does not cause any impact on the degree of perfection of the crystals. By taking $\sigma_e = 40$ ergs/cm^2,[42] σ_e reduced from 13.1, 12.4, 11.4, 10.9, 10.5, to 9.9 ergs/cm^2 for 0 wt %, 1.2 wt %, 2.4 wt %, 3.6 wt %, 4.8 wt %, 9.1 wt % nanoplate loadings. Because σ is inversely proportional to C_∞,[16] the depression of σ with increasing weight fraction of nanoplates suggested that the nanoplates facilitated the PEO chain extension. It has to point out that σ_e depends on the competition between the nucleating effect and confined segmental motions. Although the assumption of constant σ_e draws a fair explanation on the change in the chain structure with the addition of nanoplates, the identical contributions of the nucleating effect and confined segmental motions on σ_e regardless of the addition of the nanoplates seems to be unreasonable.

The other possible variation of $\sigma\sigma_e$ is the change in both σ and σ_e with the presence of nanoplates. Qiao reported a reduction of both σ and σ_e in silk fibroin fiber-reinforced poly(ε-caprolactone) biocomposites with increasing filler fraction.[45] They found that σ was nearly unchanged, but σ_e showed a remarkably depression with an increase in the filler content. From our current experimental data, it is difficult to justify the actual molecular mechanism occurred during crystallization of PEO/nanoplate composites. Further studies, such as the extraction of σ_e from Gibbs-Thomson model,[46] can facilitate to understand the crystallization mechanism of these composites.

A few researches were performed to understand the effect of fillers on the isothermal crystallization of polymer. In some composite systems, the presence of fillers acts as a nucleation agent to promote the nucleation of polymer crystallization. On the contrary, some reports proposed an antinucleation effect of fillers on polymer crystallization. This suggests that the crystallization behavior of polymer composites containing particles with different shapes and sizes cannot easily be predicted. It is worth noting that some work suggested the importance of molecular interaction between the matrix and fillers on polymer crystallization. In our work, the ionic surfactant (C_{16}TAB) acts as a surfactant to aid the uniform dispersion of nanoplates in PEO. To have more insight into the crystallization of our composite system, isothermal crystallization was performed on PEO with the presence of C_{16}TAB only. Our results revealed that the spherulite growth rate of PEO at 43°C slightly reduced from 5.38 μm/s in neat PEO to 5.10 μm/s with 1.2 wt % C_{16}TAB, 4.98 μm/s with 4.8 wt % C_{16}TAB, and 3.69 μm/s with 9.1 wt % C_{16}TAB. This indicated that the presence of C_{16}TAB dilutes the crystallites at the crystal growth front, causing the depression in the spherulite growth rate. However, we have to point out that because the volume of silver nanoplates is much smaller than that of C_{16}TAB, the addition of silver nanoplates less than 10 wt % would not cause big dilution effect on PEO crystallization. Additionally, the amount of C_{16}TAB adsorbed on nanoplates characterized from TGA is ~30%. Thus, the presence of C_{16}TAB in PEO/9.1 wt % nanoplate composites is only 2.7 wt %. This small amount of C_{16}TAB seems not to cause a significant change in the crystallization character of PEO. Similar results were proposed in the PEO crystallization with the addition of other surfactants, including sodium dodecyl sulfate (SDS) and didecyldimethylammonium bromide (DDAB).[47] Therefore, this suggested that the unique size and shape of nanoplates plays a key role on hindering the primary nucleation of PEO and increasing the spherulite growth rate.

CONCLUSIONS

The effect of two dimensional nanoplates on the isothermal crystallization of PEO was investigated. It was obtained that the incorporation of silver nanoplates into PEO caused an increase in the spherulite growth rate. However, the silver nanoplates also disrupted the nucleation of PEO. This result suggested that silver nanoplates act as an antinucleation agent in the crystallization of composites. By analyzing the radius growth rate of PEO crystallization using the Lauritzen-Hoffman's theory, we found that both K_g and $\sigma\sigma_e$ decreased with the addition of nanoplates. With the lack of the actual changes in σ and σ_e, we proposed the possible crystallization mechanisms in these PEO/nanoplate composites. A controlled experiment showed a minor change in PEO crystallization with the presence of a surfactant C_{16}TAB. This implied that the unique size and shape of nanoplates plays a key role on hindering the primary nucleation of PEO and increasing the spherulite growth rate.

References

1. Jog, J. P. Mater Sci Technol 2006, 22, 797.
2. Fornes, T. D.; Paul, D. R. Polymer 2003, 44, 3945.
3. Strawhecker, K. E.; Manias, E. Chem Mater 2003, 15, 844.
4. Bhattacharya, A. R.; Sreekumar, T. V.; Liu, T.; Kumar, S.; Ericson, L. M.; Hauge, R. H.; Smalley, R. E. Polymer 2003, 44, 2373.
5. Valentini, L.; Biagiotti, J.; Kenny, J. M.; Santucci, S. Compos Sci Technol 2003, 63, 1149.
6. Manchado, M. A. L.; Valentini, L.; Biagiotti, J.; Kenny, J. M. Carbon 2005, 43, 1499.
7. Kennedy, M.; Turturro, G.; Brown, G. R.; Stpierre, L. E. Nature 1980, 287, 316.
8. Burke, M.; Young, R. J.; Stanford, J. L. Polym Bull 1993, 30, 361.
9. Raimo, M.; Martuscelli, E. J Appl Polym Sci 2003, 90, 3409.
10. Wang, K.; Wu, J. S.; Zeng, H. M. Eur Polym Mater 2003, 39, 1647.
11. Yang, F.; Ou, Y.; Yu, Z. J Appl Polym Sci 1998, 69, 355.
12. Hoffman, J. D.; Lauritzen, J. I. J Res Natl Bur Stand A 1961, 65, 297.
13. Hoffman, J. D. SPE Transact 1964, Oct., 315.
14. Hoffman, J. D.; Miller, R. L. Polymer 1997, 38, 3151.
15. Hoffman, J. D.; Miller, R. L. Macromolecules 1988, 21, 3038.
16. Hoffman, J. D.; Miller, R. L.; Marand, H.; Roitman, D. B. Macromolecules 1992, 25, 2221.
17. Hoffman, J. D. Polymer 1991, 32, 2828.
18. Lovinger, A. J.; Davis, D. D. J Appl Phys 1985, 58, 2843.
19. Hoffman, J. D.; Lauritzen, J. I. J Appl Phys 1973, 44, 4340.
20. Hoffman, J. D.; Frolen, L. J.; Ross, G. S.; Lauritzen, J. I. J Res Natl Bur Stand A 1975, 79, 671.
21. Hoffman, J. D.; Guttman, C. M.; DiMarzio, E. A. Faraday Discuss Royal Soc Chem 1979, 68, 177.
22. Hoffman, J. D. Polymer 1983, 24, 3.
23. Snyder, C. R.; Marand, H. Macromolecules 1997, 30, 2759.
24. Heberer, D. P.; Cheng, S. Z. D.; Barley, J. S.; Lien, S. H. S.; Bryant, R. G.; Harris, F. W. Macromolecules 1991, 24, 1890.
25. Xu, J. N.; Srinivas, S.; Marand, H.; Agarwal, P. Macromolecules 1998, 31, 8230.
26. Lee, C. L.; Tseng, C. M.; Wu, R. B.; Yang, K. L. Nanotechnology 2008, 19, 215709.
27. Schultz, J. M. Polymer 1991, 32, 3268.
28. Kim, S. H.; Ahn, S. H.; Hirai, T. Polymer 2003, 44, 5625.
29. Cheng, S. Z. D.; Chen, J.; Janimak, J. J. Polymer 1990, 31, 1018.
30. Talibuddin, S.; Wu, L.; Runt, J.; Lin J. S. Macromolecules 1996, 29, 7527.
31. Alfonso, G. C.; Russell, T. P. Macromolecules 1986, 19, 1143.
32. Mucha, M.; Krolikowski, Z. J Therm Anal Calorim 2003, 74, 549.
33. Wang, T. T.; Nishi, T. Macromolecules 1977, 10, 421.
34. Buckley, C. P.; Kovacs, A. J Prog Colloid Polym Sci 1975, 58, 44.
35. Raka, L.; Sorrentino, A.; Bogoeva-Gaceva, G. J Polym Sci Polym Phys 2010, 48, 1927.
36. Causin, V.; Yang, B.-X.; Marega, C.; Goh, S. H.; Marigo, A. Euro Polym J 2009, 45, 2155.
37. Li, J.; Fang, Z.; Zhu, Y.; Tong, L.; Gu, A.; Liu, F. J Appl Polym Sci 2007, 105, 3531.
38. Abraham, T. N.; Ratna, D.; Siengchin, S.; Karger-Kocsis, J. Polym Eng Sci 2008, 49, 379.
39. Kovacs, A. J.; Straupe, C.; Gonthier, A. J Polym Sci Polym Symp 1977, 59, 31.
40. Hsu, S.-F.; Wu, T.-M.; Liao, C.–S. J Polym Sci Polym Phys 2006, 44, 3337.
41. Wu, T. M.; Chen E.-C. Polym Eng Sci 2006, 46, 1310.
42. Wu, L.; Lisowski, M.; Talibuddin, S.; Runt, J. Macromolecules 1999, 32, 1576.
43. Kim, J. Y.; Kim, S. H.; Kang, S. W.; Chang, J. H.; Ahn, S. H. Macromol Res 2006, 14, 146.
44. Krikorian, V.; Pochan, D. J. Macromolecules 2004, 37, 6480.
45. Qiao, X.; Li, W.; Sun, K.; Xu, S.; Chen, X. Polym Int 2009, 58, 530.
46. Wunderlich, B. Macromolecular Physics; Academic Press: New York, 1980.
47. Chatterjee, T.; Yurekli, K.; Hadjiev, V. G.; Krishnamoorti, R. Adv Funct Mater 2005, 15, 1832.